Experimental investigation of myocardial hypertrophy in health and disease

PhD theses

Balázs Tamás Németh, MD

Semmelweis University
Doctoral School of Basic Medicine

Tutor:

Tamás Radovits, M.D., Ph.D., associate professor

Opponents:

Attila Borbély, M.D., Ph.D., associate professor
Levente Kiss, M.D., Ph.D., assistant professor

Head of the Final Examination Committee:

Emil Monos, M.D., D.Sc., professor emeritus

Members of the Final Examination Committee:

Anikó Görbe, M.D., Ph.D., associate professor
Csaba Csonka, M.D., Ph.D., senior research fellow

Budapest
2019

Introduction

The vast majority of adult mammalian cardiomyocytes are terminally differentiated and therefore do not proliferate under physiological conditions. The heart still retains its capability to respond to environmental demands, and cardiomyocytes can grow in reaction to various physiological or pathological stimuli. Primary triggering events for cardiac hypertrophy are mechanical stress and neurohumoral stimulation, which induce various cellular responses including changes in gene expression, protein synthesis and cell metabolism, leading to the development and progression of cardiac hypertrophy. Growth of the body, pregnancy or physical exercise induces physiological enlargement of the heart, which occurs through hypertrophy of the individual cardiomyocytes, and is characterized by normal or enhanced contractility coupled with normal architecture and organization of cardiac structure. In contrast, pathological cardiac hypertrophy is associated with hemodynamic overload, injury and loss of cardiomyocytes resulting in cardiac remodeling. The occurring pathophysiological changes include, but are not limited to metabolic derangement, altered calcium handling, inflammation, cell death and fibrosis. Although pathological and physiological myocardial hypertrophy might appear to be similar phenotypically, it has long been known that they differ fundamentally in the signaling pathways that drive their development.

The mortality share of cardiovascular diseases has continuously been increasing for decades, now accounting for approximately 40% of deaths caused by non-communicable diseases worldwide. Long standing pathological hypertrophy is a major underlying cause of heart failure (HF), treatment of which is still a major healthcare problem. Therefore, new

therapeutic approaches might be feasible in addressing the growing public health burden of HF.

A feasible option to improve outcomes of HF patients might be to target and alter molecular pathways currently not involved in pharmacological therapies. Such an interesting target is the second messenger cyclic GMP (cGMP) and its downstream signaling in cardiomyocytes. cGMP generated in response to nitric oxide (NO) production is an important intracellular regulator of many physiological and pathophysiological processes in the cardiovascular system, including cardiac remodeling. It has previously been shown that elevated cytosolic levels of cGMP originated either from blockade of its degrading enzyme, phosphodiesterase type 5 (PDE-5) or from increasing its production by stimulating or activating its producing enzyme, soluble guanylate cyclase (sGC) preserved myocardial structure and function in experimental ischemia-reperfusion models. Therefore, elevating myocardial cGMP levels might prove to be an effective new method of preventing the development of pathological myocardial hypertrophy.

A new group of drugs named sGC activators has been developed in order to counteract the impairment of the NO-cGMP pathway. Cinaciguat (BAY 58-2667) is the most potent member of the sGC activators developed to this date, which is capable of activating even inactive forms of sGC, thereby increasing production of cGMP. As such, cinaciguat might become a useful novel drug in the treatment of pathological myocardial hypertrophy.

Objectives

Although both physiological and pathological myocardial hypertrophy have been extensively studied from molecular viewpoints, functional data regarding the differences between these hypertrophic phenotypes is limited in terms of reliability, given the non-invasive and thus less accurate modalities used to describe them. Therefore, there is a need to provide a deeper insight into the functional alterations characterizing these distinct forms of cardiac hypertrophy. Furthermore, since the incidence of heart failure is continuously rising, largely because of the growing incidence of its preceding conditions such as longstanding hypertension, investigation of novel pharmacological therapeutic options is of prime importance.

Our aims for the experimental investigations discussed in this thesis were as follows:

(1) Compare the functional characteristics of physiological and pathological myocardial hypertrophy utilizing pressure-volume (P-V) analysis, the current gold standard method for *in vivo* cardiac functional measurements

(2) Explore the morphological and molecular background of the functional differences observed in physiological and pathological myocardial hypertrophy

(3) Characterize the effect of the sGC activator cinaciguat in pathological myocardial hypertrophy from morphological, functional and molecular points of view as well.

Materials and methods

Model of physiological hypertrophy – exercise training

Young, male Wistar rats were randomly divided to either swim-trained (Ex) or sedentary (Sed) groups. Exercised rats performed gradually increasing training sessions until achieving 200 minutes/day for 12 weeks. Sedentary rats swam 5 minutes every day.

Model of pathological hypertrophy – pressure overload

Rats underwent either banding of the abdominal aorta (AAB) between the renal arteries and the superior mesenteric artery using a 20G needle to standardize the aortic diameter left behind, or sham procedure (Sham). Functional measurements were performed 6 weeks after the operations.

Experimental protocols

Investigation of differences between physiological and pathological myocardial hypertrophy was conducted utilizing both models. Rats (Ex, n=12; Sed, n=11; AAB, n=10; Sham, n=8) underwent the training program or the banding procedure and observation, at the end of which echocardiographic and invasive hemodynamic measurements were performed.

For the investigation of the effect of cinaciguat on pathological myocardial hypertrophy, AAB and Sham animals were randomly assigned to either receiving cinaciguat (Cin, 10mg/kg) or placebo (Co, 0.5% methylcellulose solution) in the following numbers: ShamCo n=8, ShamCin n=8, AABCo n=10, AABCin n=9. Echocardiographic images were taken at midterm (3rd week) as well as at the end of the study before invasive hemodynamic measurements.

Echocardiography

Short- and long axis images of the left ventricle (LV) were stored and analyzed to compare anterior and posterior wall dimensions as well as chamber diameters in both systole and diastole. Stroke volume (SV), fractional shortening (FS), ejection fraction (EF) and estimated LV mass index (LVMi, LV mass normalized to the tibia length of the animal) were calculated utilizing the recordings.

***In vivo* hemodynamic measurements**

Rats were anesthetized with pentobarbital sodium to carry out invasive hemodynamic measurements with a pressure-conductance microcatheter inserted into the LV after measuring mean arterial pressure (MAP). Data recorded during these measurements was used to perform P-V analysis, during which the following parameters were calculated: EF, LV end-systolic pressure (LVESP), LV end-systolic volume (LVESV), stroke work (SW), ventriculo-arterial coupling (VAC), mechanical efficiency (Eff), slope of end-systolic pressure-volume relationship (ESPVR), end-systolic elastance (E_{es}), preload recruitable stroke work (PRSW) and time constant of LV pressure decay (τ_W, Weiss method). Afterwards, hearts were weighed on a scale and LV samples collected.

Histology

Heart samples placed in 4% buffered paraformaldehyde were sectioned 5µm thick and stained with hematoxylin and eosin or Picrosirius red to determine average LV cardiomyocyte diameter and myocardial collagen content, respectively. Furthermore, cGMP immunostaining as well as terminal deoxynucleotidil transferase dUTP nick-end labeling (TUNEL) were performed to assess LV myocardial cGMP content and DNA fragmentation, respectively.

Biochemical measurement

Plasma cGMP level was determined from blood samples of ShamCo, ShamCin, AABCo and AABCin animals.

Myocardial mRNA and protein analysis

mRNA and proteins were extracted from LV samples for polymerase chain reaction and Western blotting studies. Expression of the following genes was investigated: atrial natriuretic peptide (ANP), myosin heavy chain isoform α and β (MHCα/β), peroxisome proliferator-activated receptor γ coactivator-1α (PGC1α), phospholamban (Pln) and sarcoplasmic and endoplasmic reticulum Ca^{2+}-ATPase isoform 2a (SERCA2a). On the protein level, protein kinase G (PKG) and phosphorylation ratio of vasodilator-stimulated phosphoprotein (VASP) were investigated. Glyceraldehyde-3-phosphate dehydrogenase (GAPDH) was used to normalize data in both types of analysis.

Statistical analysis

Student's *t*-testing or two-factorial analysis of variance (ANOVA, with 'aortic banding' and 'cinaciguat treatment' as factors) was carried out as appropriate. The two-factorial ANOVA was used to detect independent effects of the factors (p_{band}, p_{treat}) and significant banding×treatment interactions (p_{int}). Tukey's *post hoc* testing was performed to evaluate differences between the groups. Paired Student's *t*-test was performed for comparing data of the echocardiographic measurements at 2 time points within a group. Furthermore, to test for the effect of the different hypertrophic stimuli in the models used (p_{diff}), a two-tailed Student's *t*-test was performed using Ex and AAB values that were normalized to their respective controls.

Results

Differences between physiological and pathological myocardial hypertrophy

Heart weight

Heart weight in both Ex and AAB animals increased significantly compared with their respective controls.

Echocardiography

Anterior and posterior wall thickness was increased in both hypertrophy models both in systole and diastole. Estimated LVM and LVMi was also increased in Ex and AAB rats compared with their respective controls. A differential effect of the hypertrophic stimulus on phenotypic changes was observed in LV end-systolic diameter (LVESD), FS and EF; while LVESD decreased and FS and EF increased in Ex animals, AAB rats expressed an inverse change in these parameters compared with the Ex group (Table 1.).

Table 1. Exercise and pathological stimuli result in similar degree of hypertrophy – echocardiographic measurements

	Sed	***Ex***	***Sham***	***AAB***	p_{diff}
LVESD (mm)	4.06±0.08	3.45±0.09*	3.99±0.17	4.22±0.11	**<0.0001**
AWTd (mm)	1.96±0.02	2.17±0.02*	1.95±0.02	2.19±0.03$^{\#}$	0.452
PWTd (mm)	1.82±0.03	1.93±0.02*	1.78±0.01	2.06±0.04$^{\#}$	**0.002**
LVM (mg)	872±14	976±11*	849±17	1031±23$^{\#}$	**0.012**
LVMi (mg/mm)	20.2±0.4	24.6±0.3*	20.2±0.3	26.0±0.7$^{\#}$	0.264
FS (%)	41.4±0.7	50.0±1.1*	41.3±2.3	40.5±1.3	**<0.0001**
EF (%)	65.5±1.3	73.0±1.3*	65.1±1.5	62.4±1.3	**<0.0001**

LVESD: LV end-systolic diameter; AWTd: anterior wall thickness in diastole; PWTd: posterior wall thickness in diastole; LVM: left ventricular mass; LVMi: LVM index (LVM normalized to tibia length); FS: fractional shortening; EF: ejection fraction; p_{diff}: p value of the difference between the models

*: $p<0.05$ vs. Sed; #: $p<0.05$ vs. Sham

Hemodynamic measurements

Ex rats displayed decreased LVESV compared with Sed animals, which accompanied by unchanged heart rate and LV end diastolic volume, resulted in increased SV, EF and SW (Figure 1 A). LV pressures were unaltered in our exercised rats. In contrast, LV volumes and thus SV and EF did not change significantly in the AAB animals compared with Sham rats. In this model, however, LVESP and, consequently, MAP significantly increased in the AAB group (Figure 1 A), leading to increased values of SW. Load-independent indices of systolic cardiac function E_{es} and PRSW showed increased contractility in both hypertrophy models (Figure 1 B).

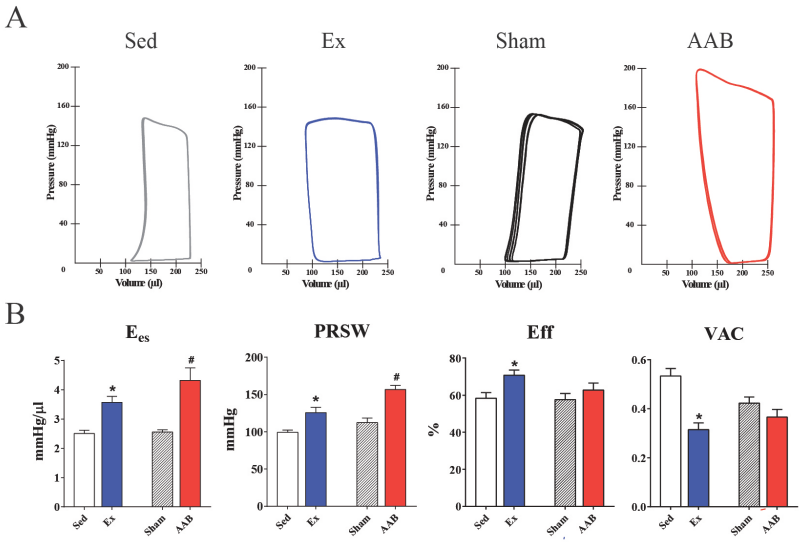

Figure 1. Pressure-volume relations and contractility following exercise or pressure overload

Panel A represents baseline P-V loops in all groups. Note the difference in pressure and volume values among the groups.
Panel B shows both E_{es} and PRSW are significantly elevated in Ex and AAB animals compared with their respective controls. Eff and VAC are significantly improved in Ex rats, while are unchanged in AAB animals.
**: p<0.05 vs. Sed; #: p<0.05 vs. Sham*

With respect to diastolic function, τ_W was significantly decreased in the Ex group compared with Sed animals, while it was significantly increased in the AAB rats compared with the Sham group. Furthermore, Eff was significantly better following exercise, while it remained unchanged after AAB. Compared with their respective controls, VAC was also improved in the Ex group, while it was mitigated in the AAB animals.

Histology

Average cardiomyocyte diameter was increased in both hypertrophy models confirming the presence of hypertrophy on the microscopic level. In contrast, while myocardial collagen content did not increase in physiological hypertrophy, pathological hypertrophy was characterized by a significant increase of subendocardial collagen deposition.

Myocardial mRNA analysis

Physical exercise did not result in significant changes regarding cardiac gene expression. In contrast, mRNA expression of genes involved in reactivation of the fetal gene program, such as ANP, MHCα and MHCβ, or expression of effectors important in mitochondrial function, such as PGC1α was altered following pressure overload of the LV.

Effects of cinaciguat in pathological myocardial hypertrophy

Heart weight

Heart weight normalized to tibia length (HW/TL) was significantly higher in the AABCo rats than in the ShamCo or ShamCin animals. HW/TL was significantly reduced in the AABCin animals compared with the AABCo rats.

Echocardiography

The echocardiographic measurement performed on the 3rd postoperative week verified significantly elevated LV wall thickness values and LVMi in the AABCo group compared with ShamCo without significant changes in chamber dimensions. LV hypertrophy increased over the second half of the treatment period in the AABCo group. Treatment with cinaciguat in aortic banded rats resulted in significantly decreased LV diastolic wall thicknesses and LVMi compared with AABCo at both time points. EF and FS remained unchanged during the whole study.

Hemodynamic measurements

LVESP and MAP proximal to the site of stenosis were significantly higher in both AAB groups than in the Sham groups, and neither of these parameters was affected by cinaciguat. ESPVR was much steeper in AABCo rats than in ShamCo animals (Figure 2 A). E_{es} and PRSW also showed that contractility was significantly elevated in the AABCo group compared with ShamCo (Figure 2 B). These parameters, however, indicated a significant decrease of contractility in AABCin compared with AABCo rats. Active relaxation was impaired in the AABCo rats compared with ShamCo, as evidenced by τ, while it was similar to ShamCo in the AABCin animals (Figure 2 B).

Histology

Average cardiomyocyte width, collagen area of subendocardial LV myocardium and the number of apoptotic cell nuclei were significantly increased in the AABCo group compared with ShamCo, and were all significantly lower in AABCin rats than in AABCo animals. Analyzing immunohistochemical staining on myocardial sections for cGMP resulted in

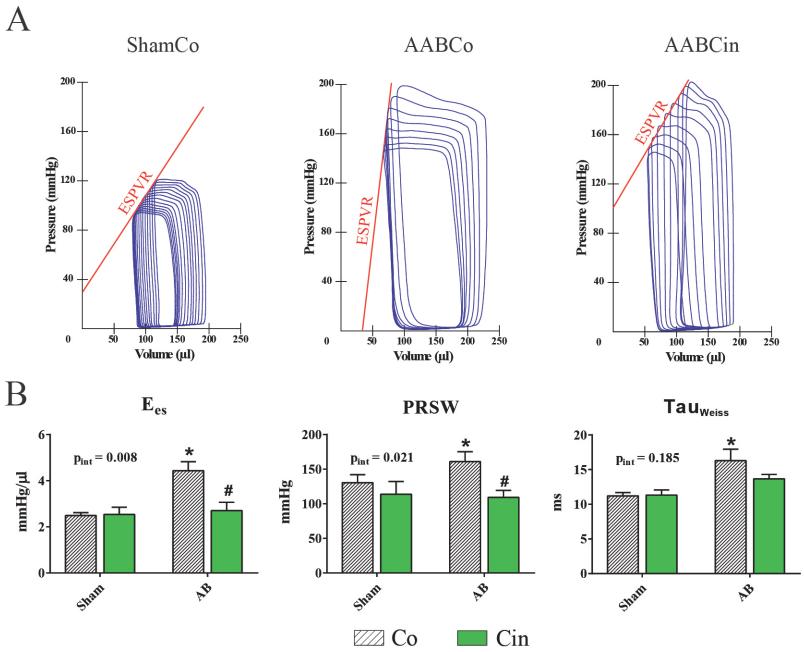

Figure 2. Pressure-volume relations and contractility following cinaciguat treatment in pressure overload

Panel A represents loops recorded during vena cava occlusion. Note the difference between ESPVR steepness.
Panel B shows both E_{es} and PRSW are significantly elevated in AABCo animals whilst both are significantly decreased in AABCin compared with AABCo. τ_W is only elevated in AABCo animals.
**: p<0.05 vs. ShamCo; #: p<0.05 vs. AABCo; p_{int}: interaction p value*

significantly higher score in AABCin rats than either in ShamCo or AABCo animals.

Myocardial mRNA and protein analysis

Pressure overload of the LV resulted in elevated myocardial expression of ANP as well as decreased ratio of MHCα/MHCβ expression, indicating the reactivation of the fetal gene program in the AABCo animals (Figure 3 A). Treatment with cinaciguat normalized the ratio of MHCα/MHCβ expression, while ANP expression was unaltered by the treatment.

Expression ratio of SERCA2a and Pln was significantly elevated in the AABCin rats (Figure 3 A). Protein density of PKG was significantly elevated in myocardial homogenates of AABCo rats, while it was comparable to ShamCo in the AABCin group (Figure 3 B). Phosphorylation ratio of VASP is a widely used indicator of PKG activity. The ratio was elevated following cinaciguat treatment in AABCin animals (Figure 3 B).

Plasma cGMP

Plasma level of cGMP was significantly elevated in the AABCin animals compared with both ShamCo and AABCo groups (Figure 3 B).

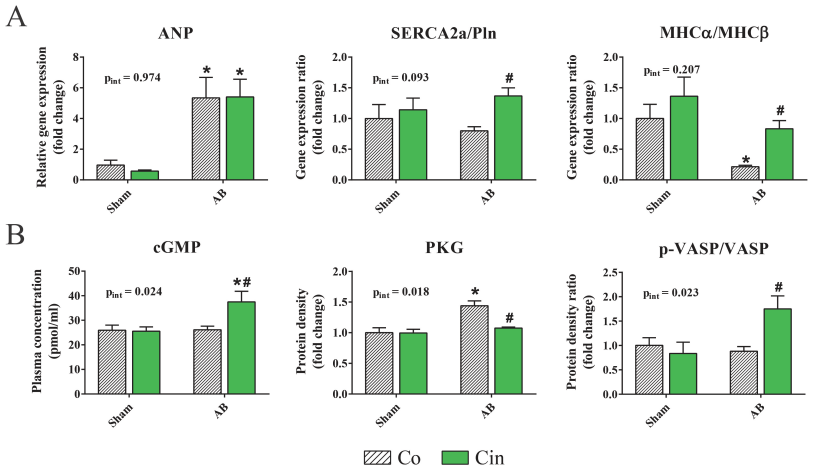

Figure 3. Gene expression changes and cGMP signaling after cinaciguat treatment in pressure overload

Panel A displays key gene expression alterations following cinaciguat treatment in pressure overload.
Panel B summarizes cGMP-related changes. Plasma level of cGMP reflects significantly higher intracellular cGMP in AABCin animals, resulting in increased PKG activity. Thus, phosphorylation ratio of VASP is increased despite the unchanged amount of the enzyme.
**: p<0.05 vs. ShamCo; #: p<0.05 vs. AABCo; p_{int}: interaction p value*

Conclusions

We provided the first detailed hemodynamic comparison of physiological and compensated pathological hypertrophy in relevant rodent models in our first set of experiments. Although the investigated types of myocardial hypertrophies were phenotypically similar, distinctive functional and molecular differences were present. Active relaxation during diastole was differentially affected: physiological hypertrophy was associated with a significant improvement, while pathological hypertrophy resulted in a significant deterioration. Furthermore, efficiency of the work of the LV and coupling to the arterial system was improved only in physiological hypertrophy. Altered myocardial expression of markers related to mitochondrial function and biogenesis might explain the described energy-dependent functional differences.

We showed for the first time in our second set of experiments that chronic activation of sGC potently prevents the development of excessive myocardial hypertrophy induced by pressure overload *in vivo*. We observed this beneficial effect of sGC activation on morphological, functional and molecular levels as well.

List of publications

Publications related to the dissertation

Németh BT, Mátyás C, Oláh A, Lux Á, Hidi L, Ruppert M, Kellermayer D, Kökény G, Szabó G, Merkely B, Radovits T. (2016) Cinaciguat prevents the development of pathologic hypertrophy in a rat model of left ventricular pressure overload. Sci Rep, 6**:** 37166.
IF_{2016}: 4.259

Oláh A, **Németh BT**, Mátyás C, Hidi L, Lux Á, Ruppert M, Kellermayer D, Sayour AA, Szabó L, Török M, Meltzer A, Gellér L, Merkely B, Radovits T. (2016) Physiological and pathological left ventricular hypertrophy of comparable degree is associated with characteristic differences of in vivo hemodynamics. Am J Physiol Heart Circ Physiol, 310**:** H587-97.
IF_{2016}: 3.348

Németh BT, Mátyás Cs, Oláh A, Lux Á, Hidi L, Ruppert M, Kellermayer D, Kökény G, Szabó G, Merkely B, Radovits T. (2017) A cinaciguat megelőzi a patológiás szívizom-hipertrófia kialakulását bal kamrai nyomás-túlterhelés patkánymodelljén. Cardiol Hung, 47**:** 183-194.

Publications not related to the dissertation

Ruppert M, Korkmaz-Icöz S, Li S, Brlecic P, **Németh BT**, Oláh A, Horváth EM, Veres G, Pleger S, Grabe N, Merkely B, Karck M, Radovits T, Szabó G. (2019) Comparison of the Reverse-Remodeling Effect of Pharmacological Soluble Guanylate Cyclase Activation With Pressure Unloading in Pathological Myocardial Left Ventricular Hypertrophy. Front Physiol, 9**:** 1869.

IF_{2017}: 3.394

Varga ZV, Erdelyi K, Paloczi J, Cinar R, Zsengeller ZK, Jourdan T, Matyas C, **Nemeth BT**, Guillot A, Xiang X, Mehal A, Hasko G, Stillman IE, Rosen S, Gao B, Kunos G, Pacher P. (2018) Disruption of renal arginine metabolism promotes kidney injury in hepatorenal syndrome. Hepatology, 68**:** 1519-1533.
IF_{2017}: 14.079

Mátyás C, Kovács A, **Németh BT**, Oláh A, Braun S, Tokodi M, Barta BA, Benke K, Ruppert M, Lakatos BK, Merkely B, Radovits T. (2018) Comparison of speckle-tracking echocardiography with invasive hemodynamics for the detection of characteristic cardiac dysfunction in type-1 and type-2 diabetes mellitus. Cardiovasc Diabetol, 17**:** 13.
IF_{2017}: 5.235

Ouyang X, Han SN, Zhang JY, **Nemeth BT**, Pacher P, Feng D, Bataller R, Cabezas J, Stärkel P, Caballeria J, LePine Pongratz R, Cai SY, Schnabl B, Hoque R, Chen Y, Yang W, Martinez IG, Wang FS, Gao B, Torok NJ, Kibbey RG, Mehal WZ. (2017) Digoxin Suppresses Pyruvate Kinase M2 Promoted HIF-1α Transactivation in Steatohepatitis. Cell Metab, 27**:** 339-350.
IF_{2017}: 20.565

Varga ZV, Matyas C, Erdelyi K, Cinar R, Nieri D, Chicca A, **Nemeth BT**, Paloczi J, Lajtos T, Corey L, Hasko G, Gao B, Kunos G, Gertsch J, Pacher P. (2018) Beta-caryophyllene protects against alcoholic steatohepatitis by attenuating inflammation and metabolic dysregulation in mice. Br J Pharmacol, 175**:** 320-334.

IF_{2017}: 6.810

Benke K, Matyas C, Sayour AA, Oláh A, **Németh BT**, Ruppert M, Szabo G, Kökény G, Horváth EM, Hartyánszky I, Szabolcs Z, Merkely B, Radovits T. (2017) Pharmacological preconditioning with gemfibrozil preserves cardiac function after heart transplantation. Sci Rep, 7**:** 14232.
IF_{2017}: 4.122

Nemeth BT, Varga ZV, Wu WJ, Pacher P. (2017) Trastuzumab cardiotoxicity: from clinical trials to experimental studies. Br J Pharmacol, 174**:** 3727-3748.
IF_{2017}: 6.810

Mátyás C, **Németh BT**, Oláh A, Török M, Ruppert M, Kellermayer D, Barta BA, Szabó G, Kökény G, Horváth EM, Bódi B, Papp Z, Merkely B, Radovits T. (2017) Prevention of the development of heart failure with preserved ejection fraction by the phosphodiesterase-5A inhibitor vardenafil in rats with type 2 diabetes. Eur J Heart Fail, 19**:** 326-336.
IF_{2017}: 10.683

Mukhopadhyay P, Horváth B, Rajesh M, Varga ZV, Gariani K, Ryu D, Cao Z, Holovac E, Park O, Zhou Z, Xu MJ, Wang W, Godlewski G, Paloczi J, **Nemeth BT**, Persidsky Y, Liaudet L, Haskó G, Bai P, Hamid Boulares A, Auwerx J, Gao B, Pacher P. (2017) PARP inhibition protects against alcoholic and nonalcoholic steatohepatitis. J Hepatol, 66**:** 589-600.
IF_{2017}: 14.911

Benke K, Sayour AA, Mátyás C, Ágg B, **Németh BT**, Oláh A, Ruppert M, Hartyánszky I, Szabolcs Z, Radovits T, Merkely B, Szabó G. (2017)

Heterotopic Abdominal Rat Heart Transplantation as a Model to Investigate Volume Dependency of Myocardial Remodeling. Transplantation, 101**:** 498-505.
IF_{2017}: 3.960

Oláh A, Kellermayer D, Mátyás C, **Németh BT**, Lux Á, Szabó L, Török M, Ruppert M, Meltzer A, Sayour AA, Benke K, Hartyánszky I, Merkely B, Radovits T. (2017) Complete Reversion of Cardiac Functional Adaptation Induced by Exercise Training. Med Sci Sports Exerc, 49**:** 420-429.
IF_{2017}: 4.291

Ruppert M, Korkmaz-Icöz S, Li S, **Németh BT**, Hegedűs P, Brlecic P, Mátyás C, Zorn M, Merkely B, Karck M, Radovits T, Szabó G. (2016) Myocardial reverse remodeling after pressure unloading is associated with maintained cardiac mechanoenergetics in a rat model of left ventricular hypertrophy. Am J Physiol Heart Circ Physiol, 311**:** H592-603.
IF_{2016}: 3.348

Matyas C, Varga ZV, Mukhopadhyay P, Paloczi J, Lajtos T, Erdelyi K, **Nemeth BT**, Nan M, Hasko G, Gao B, Pacher P. (2016) Chronic plus binge ethanol feeding induces myocardial oxidative stress, mitochondrial and cardiovascular dysfunction, and steatosis. Am J Physiol Heart Circ Physiol, 310**:** H1658-1670.
IF_{2016}: 3.348

Mátyás Cs, **Németh BT**, Oláh A, Hidi L, Birtalan E, Kellermayer D, Ruppert M, Korkmaz S, Kökény G, Horváth EM, Szabó G, Merkely B, Radovits T. (2015) The soluble guanylate cyclase activator cinaciguat

prevents cardiac dysfunction in a rat model of type-1 diabetes mellitus. Cardiovasc Diabetol, 14**:** 145.
IF_{2015}: 4.534

Kovács A, Oláh A, Lux Á, Mátyás Cs, **Németh BT**, Kellermayer D, Ruppert M, Török M, Szabó L, Assabiny A, Birtalan E, Merkely B, Radovits T. (2015) Strain and strain rate by speckle tracking echocardiography correlate with pressure-volume loop derived contractility indices in a rat model of athlete's heart. Am J Physiol Heart Circ Physiol, 308**:** H743-748.
IF_{2015}: 3.324

Oláh A, **Németh BT**, Mátyás Cs, Horváth EM, Hidi L, Birtalan E, Kellermayer D, Ruppert M, Merkely G, Szabó G, Merkely B, Radovits T. (2015) Cardiac effects of acute exhaustive exercise in a rat model. Int J Cardiol, 182**:** 258-266.
IF_{2015}: 4.638

Radovits T, Korkmaz S, Mátyás Cs, Oláh A, **Németh BT**, Páli Sz, Hirschberg K, Zubarevich A, Gwanmesia PN, Li S, Loganathan S, Barnucz E, Merkely B, Szabó G. (2014) An altered pattern of myocardial histopathological and molecular changes underlies the different characteristics of type-1 and type-2 diabetic cardiac dysfunction. J Diabetes Res, 2015**:** 728741.
IF_{2015}: 2.431

Weymann A, Radovits T, Schmack B, Korkmaz S, Li S, Chaimow N, Pätzold I, Becher PM, Hartyánszky I, Soós P, Merkely G, **Németh BT**, Istók R, Veres G, Merkely B, Terytze K, Karck M, Szabó G. (2014) Total

aortic arch replacement: Superior ventriculo-arterial coupling with decellularized allografts compared with conventional prostheses. PLoS One, 9**:** e103588.
IF_{2014}: 3.234

Radovits T, Oláh A, Lux A, **Németh BT**, Hidi L, Birtalan E, Kellermayer D, Mátyás C, Szabó G, Merkely B. (2013) Rat model of exercise-induced cardiac hypertrophy - hemodynamic characterization using left ventricular pressure-volume analysis. Am J Physiol Heart Circ Physiol, 305**:** H124-134.
IF_{2013}: 4.012

Oláh A, Sayour AA, **Németh BT**, Mátyás Cs, Hidi L, Lux Á, Ruppert M, Kellermayer D, Szabó L, Török M, Meltzer A, Gellér L, Merkely B, Radovits T. (2018) A hasonló fokú fiziológiás és patológiás balkamra-hipertrófia különböző in vivo hemodinamikai következményekhez vezet. Cardiol Hung, 48**:** 20-30.

Ruppert M, Barta B, Korkmaz-Icöz S, Li S, Oláh A, Mátyás Cs, **Németh BT**, Benke K, Sayour AA, Karck M, Merkely B, Radovits T, Szabó G. (2018) A hipertrófiás myocardium reverz elektromos remodellációjának vizsgálata patkánymodellben. Cardiol Hung, 48**:** 118-128.

Mátyás Cs, Sayour A, Korkmaz-Icöz S, Oláh A, **Németh BT**, Páli Sz, Hirschberg K, Zubarevich A, Gwanmesia PN, Li S, Loganathan S, Barnucz E, Merkely B, Szabó G, Radovits T. (2017) Az 1-es és 2-es típusú diabéteszes kardiális diszfunkció hátterében álló eltérő miokardiális szövettani és molekuláris jellegzetességek. Cardiol Hung, 47**:** 102-111.

Mátyás Cs, Barta B, **Németh BT**, Oláh A, Hidi L, Birtalan E, Kellermayer D, Ruppert M, Korkmaz-Icöz S, Kökény G, Horváth EM, Szabó G, Merkely B, Radovits T. (2017) A szolubilis guanilát-cikláz aktivátor cinaciguat megelőzi a kardiális diszfunkció kialakulását 1-es típusú cukorbetegség patkánymodelljében. Cardiol Hung, 47**:** 34-45.

Benke K, Sayour AA, Ágg B, Radovits T, Szilveszter B, Odler B, **Németh BT**, Pólos M, Oláh A, Mátyás Cs, Ruppert M, Hartyánszky I, Maurovich-Horvat P, Merkely B, Szabolcs Z. (2016) Génpolimorfizmusok, mint rizikófaktorok a Marfan-szindróma kardiovaszkuláris manifesztációinak előrejelzésében. Cardiol Hung, 46**:** 76-81.

Oláh A, **Németh BT**, Mátyás Cs, Horváth EM, Hidi L, Birtalan E, Kellermayer D, Ruppert M, Gellér L, Szabó G, Merkely B, Radovits T. (2016) Az egyszeri, kimerítő fizikai terhelés kardiális hatásainak vizsgálata patkánymodellen. Cardiol Hung, 46**:** 1-9.

Oláh A, Lux Á, **Németh BT**, Hidi L, Birtalan E, Kellermayer D, Mátyás C, Ruppert M, Merkely G, Szabó G, Merkely B, Radovits T. (2013) A sportszív részletes hemodinamikai jellemzése bal kamrai nyomás-térfogat analízis segítségével. Cardiol Hung, 43**:** 224-232.

Németh BT, Hidi L, Tóth R, Radovits T, Szabó G, Merkely B, Horkay F, Veres G. (2013) A szívizomvédelem lehetőségei a szívsebészeti gyakorlatban. Cardiol Hung, 43**:** 63-69.